J Fluoresc (2012) 22:891–897
DOI 10.1007/s10895-011-1027-8

ORIGINAL PAPER

Synthesis and Luminescent Properties of $M_2V_2O_7$: Eu (M=Sr, Ba) Nanophosphors

Sheetal · V. B. Taxak · S. P. Khatkar

Received: 16 October 2011 / Accepted: 19 December 2011 / Published online: 30 December 2011

Abstract A solution combustion route for the synthesis of Eu^{3+}-activated $M_2V_2O_7$ (M = Sr, Ba) and their luminescent properties have been investigated. Structure and luminescent characteristics of $Sr_2V_2O_7$:Eu^{3+} and $Ba_2V_2O_7$:Eu^{3+} nanophosphors have been studied by x-ray diffraction, scanning electron microscopy, transmission electron microscopy, fluorescence spectrometry and Fourier transform infra-red spectroscopy. The incorporation of Eu^{3+} activator in these nanoparticles has been checked by luminescence characteristics. These nanoparticles have displayed red color under a UV source which is due to characteristics transition of Eu^{3+} from $^5D_0 \rightarrow {}^7F_2$ at 613 nm in both $Sr_2V_2O_7$:Eu^{3+} and $Ba_2V_2O_7$:Eu^{3+} nanophosphors. In addition, the optimal Eu^{3+} - doped contents of $Sr_{2(1-x)}Eu_{2x}V_2O_7$ and $Ba_{2(1-x)}Eu_{2x}V_2O_7$ nanophosphors for both were 4 mol%.

Keywords Nanophosphor · Luminescence · $Sr_2V_2O_7$: Eu · $Ba_2V_2O_7$: Eu

Introduction

Rare earth doped compounds have been widely applied in the fields of high-performance luminescent devices, catalysts and other functional materials due to their exceptional electronic, optical and chemical characteristics arising from 4f electrons [1–5]. Vanadium oxide compounds are widely used as multifunctional optical materials: phosphors, luminescent indicators, thermoluminescent detectors, lasing media, scintillators etc. [6]. Meta-, pyro- and orthovanadates offer efficient intrinsic luminescence due to the vanadium-oxygen groups in their crystal structures [7]. To find novel efficient white light emitting diodes (LEDs) phosphors, europium has been the focus of attention for the researchers as an activator because of its strong red emission. Eu^{3+} doped phosphors can be effectively excited by near-UV and blue light and then emit stronger red fluorescence attributable to the $^5D_0 \rightarrow {}^7Fj$ (j=0–4) transitions [8].

$Sr_2V_2O_7$ and $Ba_2V_2O_7$ are member of a series of luminescent materials with general formula $M_2V_2O_7$ (M = Mg, Ca, Sr, Ba, Zn, Cd, Hg). Many polycrystalline pyrovanadates $M_2V_2O_7$ (M = Ca, Sr, Ba) having triclinic and hexagonal structures [9–12] have been investigated to have a rare luminescent property and these compounds showed a quite broad band luminescence in the visible range from 400 to 800 nm derived from the CT transition in the VO_4 tetrahedra. The broad band luminescence in the visible region is effective to obtain a good color rendering property for the light devices. Fluorescence studies on $M_2V_2O_7$ (M = Ca, Sr, Ba) have been reported by Nakajima [13] and luminescent color of these new vanadate phosphor system varied from green (M: Ba) to yellowish orange (M: Ca) with internal quantum efficiency (η) 25%, 8% and 0.9% respectively. Thermal stability and pulsed cathodoluminescence properties of potassium strontium vanadates were studied by Slobodin et al. [7]. Luminescent properties and different morphologies of $Ca_2V_2O_7$:Eu^{3+} using different surfactants were investigated by J. Gu and B. Yan [14]. Recently, $Sr_2V_2O_7$ nanoribbons were synthesized via a hydrothermal process [15]. But to our best knowledge there are no reports on $M_2V_2O_7$: Eu^{3+} (M = Sr, Ba) nanophosphors synthesis.

Solution combustion synthesis (SCS) has emerged as an attractive technique for the synthesis of high purity

Sheetal · V. B. Taxak · S. P. Khatkar (✉)
Department of Chemistry, Maharshi Dayanand University, Rohtak 124001, India
e-mail: s_khatkar@rediffmail.com

homogeneous and crystalline oxide powders at significantly lower temperatures than the conventional synthesis method, because the starting raw materials are homogeneously mixed in liquid phase and the high temperature generated instantly by the exothermic radiation can volatilize low boiling point impurities [16–19]. The attractive features of SCS are its ability to synthesize materials with high purity, better homogeneity and high surface area in a single step. As a part of our programme on luminescent materials [20–22], here we report the use of solution combustion synthesis (SCS) for the preparation of Eu^{3+}-doped $Sr_2V_2O_7$ and $Ba_2V_2O_7$ nanophosphors.

Experiment

The starting reagents were high purity $Sr(NO_3)_2$, $Ba(NO_3)_2$, NH_4VO_3, $Eu(NO_3)_3.5H_2O$ and urea. According to nominal composition of $Sr_{2(1-x)}V_2O_7{:}2xEu^{3+}$ (x=0.005, 0.02, 0.04, 0.05), a stoichiometric amount of metal nitrates were dissolved in minimum quantity of deionized water in 200 mL capacity pyrex beaker. Then urea was added in this solution with molar ratio of urea to nitrates based on total oxidizing and reducing valencies of oxidizer and the fuel (urea) according to concept used in propellant chemistry [23]. Finally the beaker containing the solution was placed into a preheated furnace at 500 °C. The material undergoes rapid dehydration and foaming followed by decomposition, generating combustible gases. These volatile combustible gases ignite and burn with a flame yielding voluminous solid. Similarly $Ba_{2(1-x)}V_2O_7{:}2xEu^{3+}$ nanoparticles were synthesized. Urea was oxidized by nitrate ions and served as a fuel for propellant reaction. Combustion synthesized nanoparticles were annealed at different temperatures from 700 °C to 900 °C in order to know the effect of annealing on the particle size/shape and luminescence properties.

Characterization

The crystal phase of $Sr_2V_2O_7{:}Eu^{3+}$ and $Ba_2V_2O_7{:}Eu^{3+}$ nanoparticles prepared were characterized by a table top Rigaku Miniflex-II X-ray powder diffraction with CuKα radiation at 30 kV tube voltage and 15 μA tube current. The particle size and morphology were evaluated using Jeol JSM-6510 scanning electron microscope (SEM) and FEI-Morgagni-268D transmission electron microscope (TEM). The excitation and emission spectra of nanoparticles in the ultraviolet–visible region were obtained by using a Hitachi F-7000 fluorescence spectrophotometer with Xe- lamp at room temperature. The Fourier transform infrared (FT-IR) spectra were recorded using a Perkin Elmer spectrometer in the spectral range 4,000–400 cm^{-1} following KBr pellet technique. The background correction has been made in the FT- IR experiment.

Results and Discussion

As like most pyro- compounds, $Sr_2V_2O_7$ is dimorphic. Their crystals are anorthic α phase with space group $P1$ at high temperature, while the other is tetragonal β phase with space group $P4_1$ at low temperature [12]. The α- to β- polymorphic transition temperature is about 645 °C. The crystal class of β- $Sr_2V_2O_7$ (tetragonal) is more symmetric than that of α-$Sr_2V_2O_7$ (anorthic), but α-$Sr_2V_2O_7$ is centric while β-$Sr_2V_2O_7$ is acentric. Kohlmuller and Perraud [24] synthesized $Ba_2V_2O_7$ and indicated that it is dimorphic. $Ba_2V_2O_7$ at higher temperature has triclinic structure with space group $P1$ [11]. The XRD patterns of solution combustion synthesized $Sr_2V_2O_7$ and $Ba_2V_2O_7$ powders doped with 4 mol% Eu^{3+} as prepared(at 500 °C) and after annealed treatment at 700 °C and 900 °C for 3 h are shown in Fig. 1a and b respectively. All diffraction peaks of $Sr_2V_2O_7$ powders annealed at 700 °C and 900 °C can be indexed to anorthic phase of $Sr_2V_2O_7$ (JCPDS card no. 81-0837). No peaks from other phases can be detected. Similarly, the diffraction peaks of $Ba_2V_2O_7$ on annealing at 700 °C and 900 °C were consistent with the literature data [11] showing a crystalline structure composed of $Ba_2V_2O_7$ powders with anorthic phase belonging to space group $P1$. In general, the intensities of XRD peaks increases with increase of annealing temperatures which indicate better crystallinity, which is reflected by the high intensity and narrower peaks of the spectra at 900 °C. XRD patterns of samples prepared at 500 °C show many additional peaks corresponding to those of pure $Sr(NO_3)_2$ phase (JCPDS card no. 004-0310) and $Ba(NO_3)_2$ phase (JCPDS card no. 004-0773) in addition to the lower temperature β phase of nanophosphors. It seems that 500 °C is not a sufficient temperature to decompose $Sr(NO_3)_2$ and $Ba(NO_3)_2$ to prepare $Sr_2V_2O_7$ and $Ba_2V_2O_7$ phase in their respective mixtures. The effect of Eu^{3+} ions concentrations (0.5, 2, 4 and 5 mol%) on $Ba_2V_2O_7$ lattice seems to be negligible as XRD patterns remain the same at different doping concentrations (Fig. 1c). Almost identical XRD patterns are obtained for samples of $Sr_2V_2O_7$ with different doping concentrations of europium. The size of the crystallites can be estimated with the help of Scherrer equation, $D=0.89\lambda/\beta\cos\theta$, where D is the average grain size, λ the X-ray wavelength (0.15418 nm), and θ and β are the diffraction angles and full-width at half-maximum (FWHM, in radian) of an observed peak, respectively[25]. The calculated average particle sizes (D) of $Sr_2V_2O_7{:}Eu^{3+}$ nanoparticles were found to be 40 nm and 47 nm at annealing temperatures 700 °C and 900 °C respectively whereas for $Ba_2V_2O_7{:}Eu^{3+}$ nanoparticles the sizes were found to be 43 nm and 51 nm at annealing temperatures 700 °C and 900 °C respectively. With the increase of temperature the crystal size becomes larger.

Figure 2 depicts the typical red photoluminescence from Eu^{3+} ions in the $Sr_2V_2O_7{:}Eu^{3+}$ and $Ba_2V_2O_7{:}Eu^{3+}$ nanoparticles when rooting the excitation wavelength at 394 nm. It is

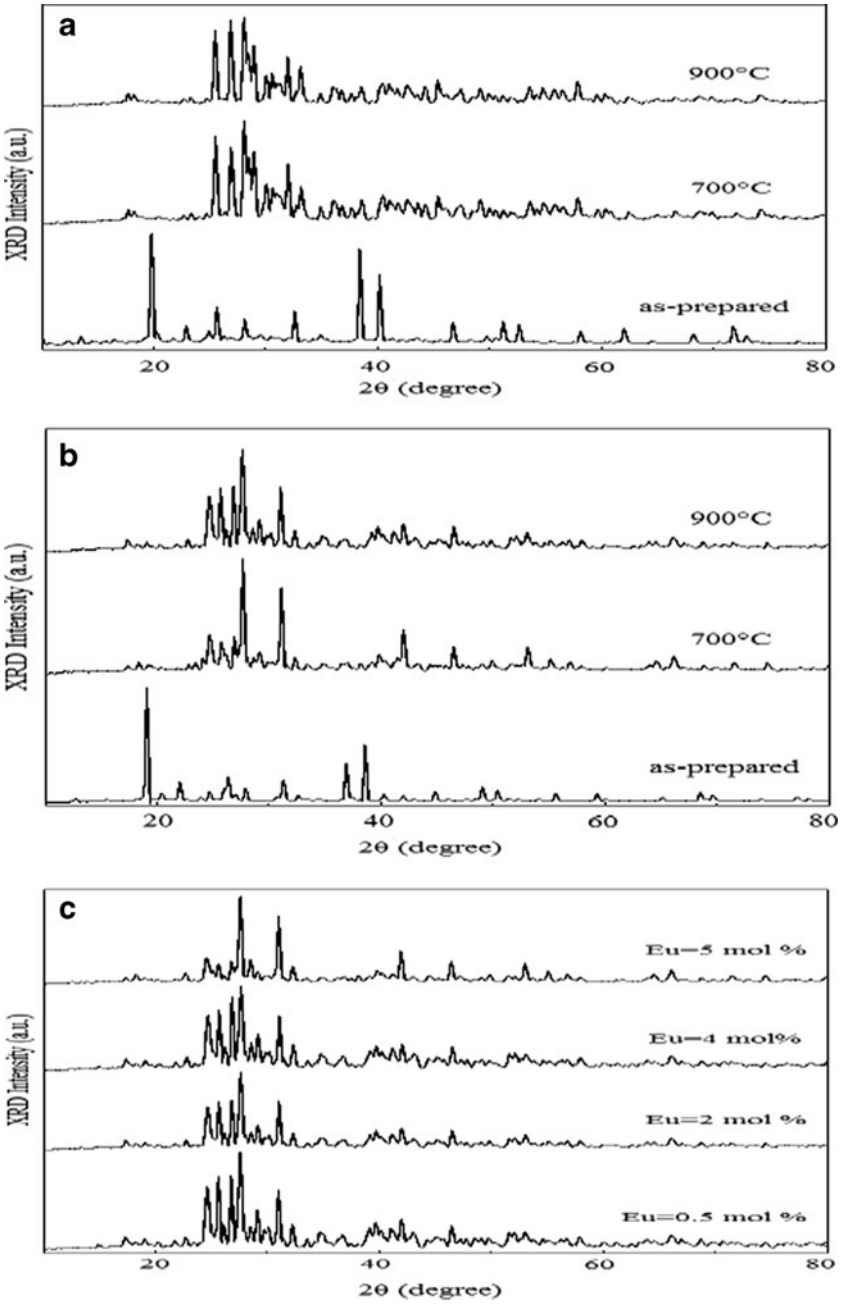

Fig. 1 XRD patterns of (**a**) $Sr_{1.92}Eu_{0.08}V_2O_7$ at different temperatures and of (**b**) $Ba_{2(1-x)}Eu_{2x}V_2O_7$ at different temperatures and (**c**) $Ba_2V_2O_7$:Eu^{3+} (Eu^{3+} = 0.5, 2, 4, 5 mol%) annealed at 900 °C

clear that the PL intensity of the as–synthesized nanophosphors at 500 °C, increased rapidly after annealing from 700 °C to 900 °C (Fig. 2a and c) in both the compounds. This is mainly due to the improvement in doping and crystallinity. In particular, the most intense emission peak at 613 nm in both $Sr_2V_2O_7$:Eu^{3+} and $Ba_2V_2O_7$:Eu^{3+} corresponds to $^5D_0 \rightarrow {}^7F_2$ and occurs through the forced electric dipole, while the $^5D_0 \rightarrow {}^7F_1$ band at 588 nm is the magnetic dipole transition [14]. The emission spectrum is dominated by $^5D_0 \rightarrow {}^7F_2$ hypersensitive transition (ΔJ=2), which is because the Eu^{3+} is located at a low symmetry local site in the $M_2V_2O_7$ (M = Sr, Ba) host lattice. Moreover, the splitting number of $^5D_0 \rightarrow {}^7F_j$ transitions can provide information of the surroundings of the Eu^{3+} ions [26, 27], and the site symmetry of Eu^{3+} ion with a maximum number of lines "2J+1" for each lattice site. Unique $^5D_0 \rightarrow {}^7F_0$ (588 nm) transition indicates that the Eu^{3+} ions occupy single sites in both $Sr_2V_2O_7$ and $Sr_2V_2O_7$ lattices. In addition, the PL intensity of $Sr_2V_2O_7$:Eu^{3+} is greater as compared to $Ba_2V_2O_7$:Eu^{3+} (Fig. 2e).

Generally, the luminescence properties of nanoparticles depend on the activator concentration and crystallinity. Dependence of the emission intensity of europium ions upon the doping concentration (x) in the crystalline $Sr_{2(1-x)}Eu_{2x}V_2O_7$ and $Ba_{2(1-x)}Eu_{2x}V_2O_7$ (900 °C annealed) excited by 394 nm is

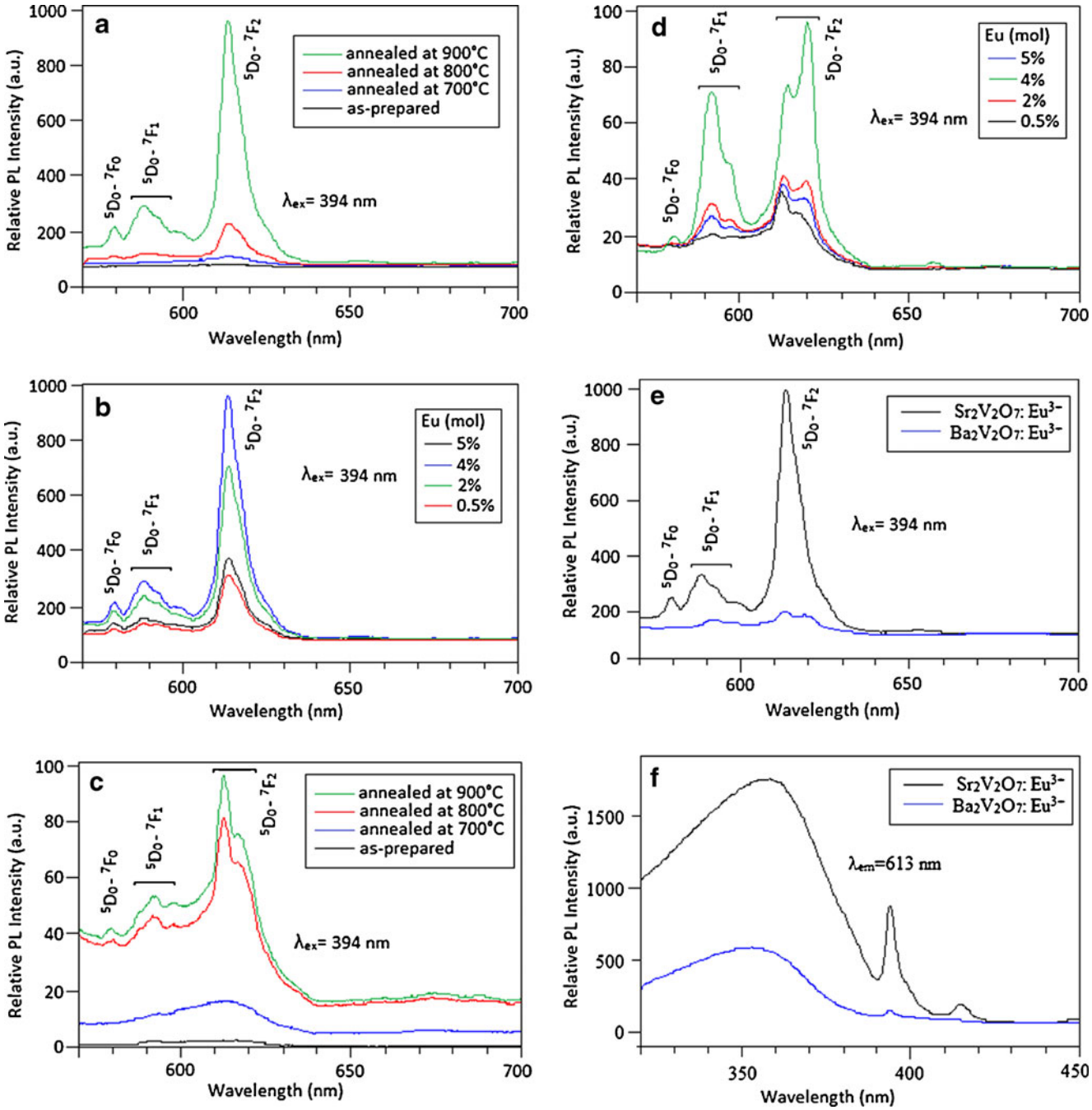

Fig. 2 Emission spectra of $Sr_{2(1-x)}Eu_{2x}V_2O_7$ (**a**) annealed at different temperatures (**b**) with different mol% doping of Eu^{3+} annealed at 900 °C; Emission spectra of $Ba_{2(1-x)}Eu_{2x}V_2O_7$ (**c**) annealed at different temperatures (**d**) with different mol% doping of Eu^{3+} annealed at 900 °C; (**e**) Comparison of emission spectra of $Sr_2V_2O_7$: Eu^{3+} and $Ba_2V_2O_7$: Eu^{3+} with 4 mol% doping of Eu^{3+} annealed at 900 °C; (f) Comparison of excitation spectra of $Sr_2V_2O_7$: Eu^{3+} and $Ba_2V_2O_7$: Eu^{3+} with 4 mol% doping of Eu^{3+} annealed at 900 °C

shown in Fig. 2b and d respectively. It is found that the PL emission intensity of Eu^{3+} increased with the increase in the concentration, reaching a maximum value with 4 mol% doping of Eu^{3+}. Usually, an over-doping concentration results in the enhancement of non-radiative relaxation between the neighboring Eu^{3+} ions which indicates the concentration quenching.

Figure 2f shows the photoluminescence excitation spectra of Eu^{3+} in $Sr_2V_2O_7$ and $Ba_2V_2O_7$ host lattices. The excitation spectra include a dominant broad region (320–390 nm) which is superimposed to Eu^{3+} absorption lines following that which are in form of a series of sharp lines beyond 390 nm. The broad peak is ascribed to charge transfer band (CTB) which corresponds to an electron

transfer from an oxygen 2p orbital to an empty 4*f* orbital of europium ions ($O^{2-} \rightarrow Eu^{3+}$). The sharp lines in the range above 390 nm are intra-configurational 4*f*-4*f* transitions of Eu^{3+} in the host lattices, peak with maxima at ~395 nm ($^7F_0 \rightarrow {}^5L_6$) being the dominating.

The morphology and particle size of the $Sr_2V_2O_7$: Eu^{3+} and $Ba_2V_2O_7$: Eu^{3+} nanoparticles both as prepared and annealed at 700 °C and 900 °C have been investigated by SEM and TEM as shown in Figs. 3 and 4. The as synthesized products by the combustion process show an unusual morphology i.e. forming cracks and porous network due to rapid release of gases by-products during the combustion. This type of porous network is typical of combustion synthesized powders. For the powder synthesized at 500 °C by combustion, the particle size was very small and the particles tend to agglomerate. With an increase of temperature, particle size increased and agglomeration decreased. The $Sr_{1.92}Eu_{0.08}V_2O_7$ and $Ba_{1.92}Eu_{0.08}V_2O_7$ nanocrystals exhibit narrow size distribution with spherical shape and slight agglomerate phenomenon with grain size in the range 40–55 nm, which is in full agreement with the data from XRD patterns.

The Fourier transform infrared (FT-IR) spectra of annealed $Sr_2V_2O_7$: Eu^{3+} and $Ba_2V_2O_7$: Eu^{3+} (Eu = 4 mol%) nanophosphors are shown in Fig. 5. Strong peaks observed in the 460–900 cm^{-1} region are due to several M-O stretching and bending vibrations. The O-V-O asymmetric vibration band is observed at 580 cm^{-1} and 564 cm^{-1} respectively whereas the V-O stretching vibration bands exist in region 930–720 cm^{-1} Beside this, the fundamental H_2O vibration modes at 3,400 cm^{-1} due to O-H stretching vibration and at 1,600 cm^{-1} due to H-O-H bending vibration

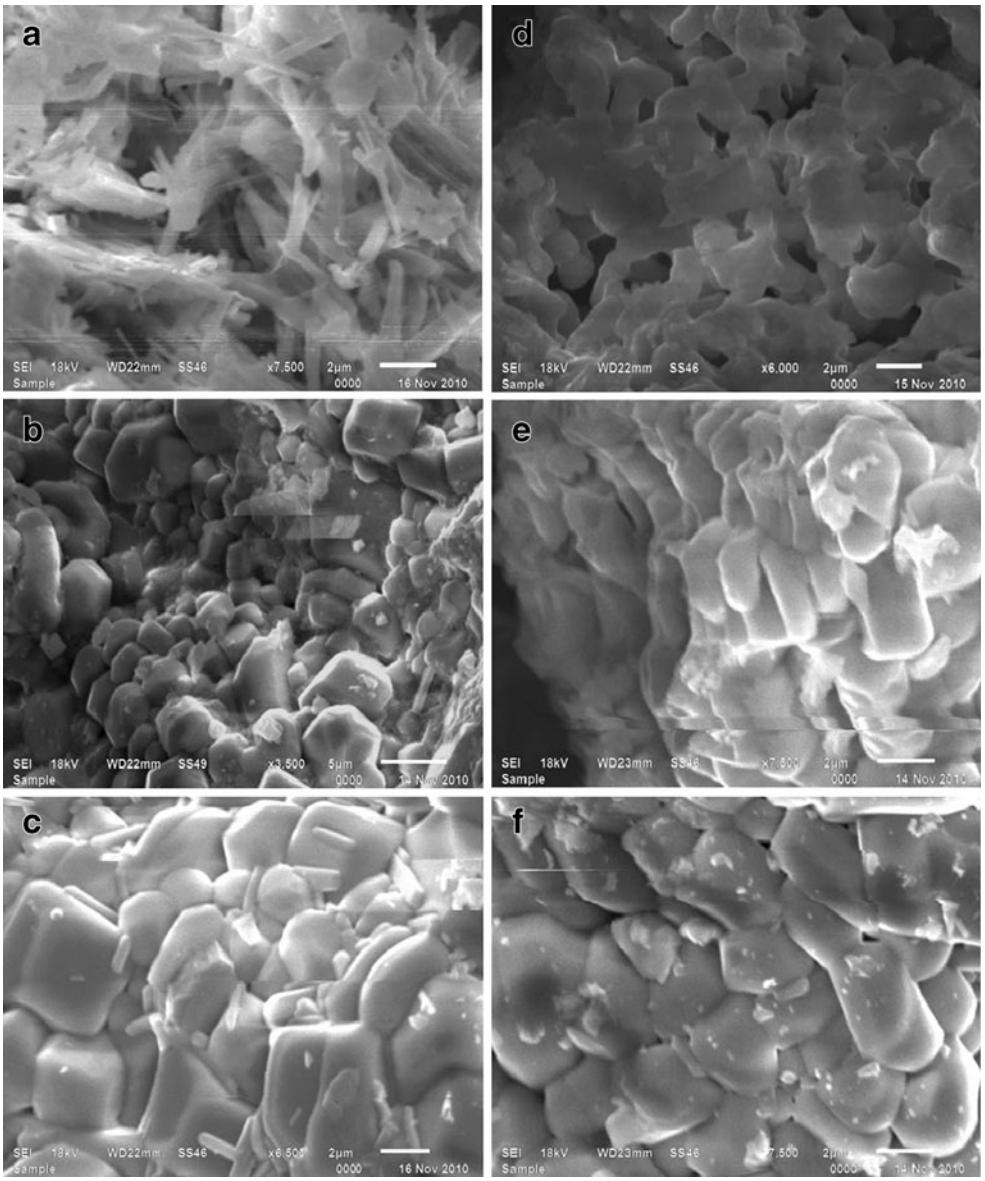

Fig. 3 SEM images of $Sr_2V_2O_7$: Eu^{3+} nanophosphors (**a**) as-prepared, annealed at (**b**) 700 °C and (**c**) 900 °C and of $Ba_2V_2O_7$: Eu^{3+} (**d**) as-prepared, annealed at (**e**) 700 °C and (**f**) 900 °C with 2 mol% doping of Eu^{3+}

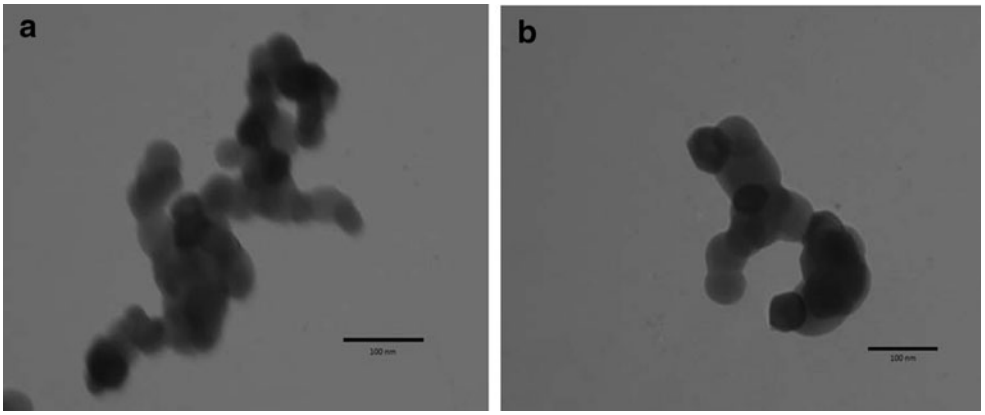

Fig. 4 TEM images of (**a**) $Sr_2V_2O_7$: Eu^{3+} annealed at 900 °C and (**b**) $Ba_2V_2O_7$: Eu^{3+} annealed at 900 °C with 4 mol% doping of Eu^{3+}

did not appear as the samples were annealed at high temperature.

Conclusion

$Sr_2V_2O_7$: Eu^{3+} and $Ba_2V_2O_7$: Eu^{3+} nanophosphors have been synthesized by the urea-assisted solution combustion synthesis. The results from TEM studies show that both $Sr_2V_2O_7$ and $Ba_2V_2O_7$ doped with Eu has a mean particle size of about 45 nm with spherical like morphology. The emission spectra were recorded under λ_{ex} =394 nm and exhibited the strongest peaks at 613 nm for both $Sr_2V_2O_7$: Eu^{3+} and $Ba_2V_2O_7$: Eu^{3+}. The $Sr_2V_2O_7$: Eu^{3+} and $Ba_2V_2O_7$: Eu^{3+} nanophosphors thus prepared show to possess red-emitting property attractive to a wide range of potential applications in electronic devices.

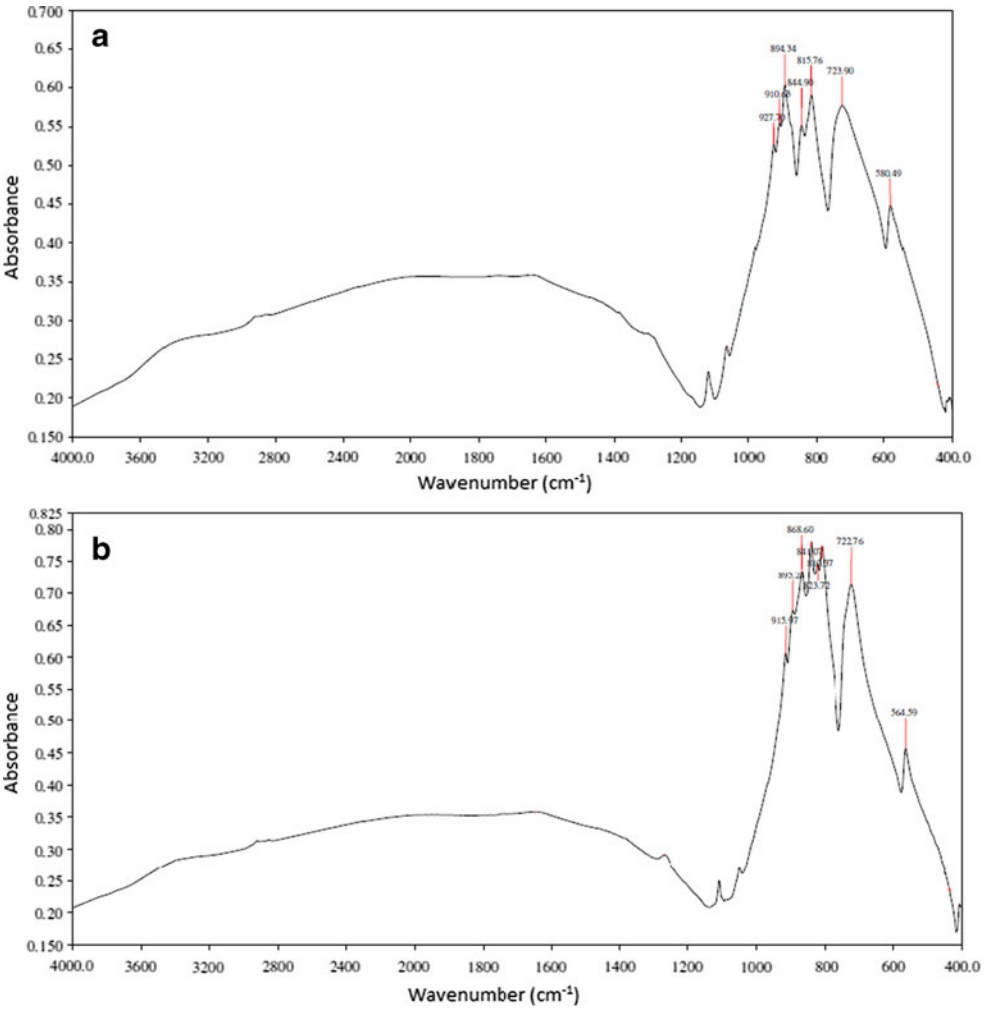

Fig. 5 FT-IR spectra of (**a**) $Sr_{2(1-x)}V_2O_7$:2xEu^{3+} and (**b**) $Ba_{2(1-x)}V_2O_7$:2xEu^{3+} with 4 mol% doping of Eu^{3+}

Acknowledgement One of the authors Ms. Sheetal gratefully acknowledges the financial support in the form of JRF (UGC) New Delhi.

References

1. Wang J, Hojamberdiev M, Xu Y, Peng J (2011) Mater Chem Phys 125:82
2. Tang Q, Liu ZP, Li S, Zhang SY, Liu XM, Qian YT (2003) J Cryst Growth 259:208
3. Capobianco JA, Vetrone F, Boyer JC, Speghini A, Bettinelli M (2002) Opt Mater 19:259
4. Palmer MS, Neurock M, Olken MM (2002) J Am Chem Soc 124:8452
5. Hasegawa Y, Thongchant S, Wada Y, Tanaka H, Kawai T, Sakata T, Mori H, Yanagida S (2002) Angew Chem 41:2073
6. Fotiev AA, Shul'gin BV, Moskvin AS, Gavrilov FF (1976) Vanadievye kristallofosfory (crystalline vanadium phsphors). Nauka, Moscow
7. Slobodin BV, Surat LL, Samigullina RF, Ishchenko AV, Cherepanov AN, Shul'gin BV (2009) Inorg Mater 45(4):428
8. Li Q, Huang J, Chen D (2011) J Alloys Compd 509:1007
9. Hawthorne FC, Calvo C (1978) J Solid State Chem 26:345
10. Huang J, Sleight AW (1992) Mater Res Bull 27:581
11. Joung M-R, Kim J-S, Song M-E, Nahm S, Paik J-H (2010) J Am Soc 93–8:2132
12. Baglio JA, Dann JN (1972) J Solid State Chem 4:87
13. Nakajima T, Isobe M, Tsuchiya T, Ueda Y, Manabe T (2010) Opt Mater 32:1618
14. Gu J, Yan B (2009) J Alloys Compd 476:619
15. Zhou Q, Shao M, Chen T, Xu H (2010) Mater Res Bull 45:1051
16. Singh V, Rai VK, Shamery KA, Nordmann J, Haase M (2011) J Lumin 131:2679
17. Jayaramaiah JR, Lakshminarasappaa BN, Nagabhushanac BM (2011) Mater Chem Phys 130:175
18. Pekgozlu I, Erdogmus E, Demirel B, Gok MS, Karabulut H, Basak AS (2011) J Lumin 131:2290
19. Chen Z, Yan Y, Liu J, Yin Y, Wen H, Zao J, Liu D, Tian H, Zhang C, Li S (2009) J Alloys Compd 473:L13
20. Taxak VB, Khatkar SP, Han S-D, Kumar R, Kumar M (2009) J Alloys Compd 469:224
21. Marí B, Singh KC, Sahal M, Khatkar SP, Taxak VB, Kumar M (2011) J Lumin 131:587
22. Marí B, Singh KC, Sahal M, Khatkar SP, Taxak VB, Kumar M (2010) J Lumin 130:2128
23. Ekambaram S, Patil KC (1997) J Alloy Comp 448:7
24. Kohlmuller R, Perraud J (1964) Bull Soc Chim Fr
25. Zeng XQ, Hong GY, You HP, Wu XY (2001) Chin J Lumin 22:58
26. Huang J, Zhou L, Wang Z, Lan Y, Tong Z, Gong F, Sun J, Li L (2009) J Alloys Compd 487:L5
27. Thim GP, Brito HF, Silva SA, Oliveira MAS, Felintoc MCFC (2003) J Solid State Chem 171:375